scientific reports

Check for updates

OPEN

Inline UV pulse synthesizer

Sung In Hwang[1,2], Wosik Cho[1,3], Hyeok Yun[2], Kyung Taec Kim[1,3], Jin Woo Yun[1,2], Seong Ku Lee[1,2] & Jae Hee Sung[1,2]✉

We demonstrated an inline synthesizer for generating ultrashort pulses in the ultraviolet (UV) range. The inline UV pulse synthesizer comprised three nonlinear crystals located in the propagation path of the fundamental driving laser pulse. Second-harmonic signals with central wavelengths of 420, 375, and 345 nm were generated in turn in the three BBO crystals, resulting in a synthesized UV pulse subsequent to the final nonlinear crystal. Its temporal amplitude and phase could be manipulated easily by changing the relative positions of the crystals, allowing for flexibility of the waveform. The minimum pulse duration of the synthesized UV pulse was 4.7 fs, which was close to the Fourier-transform-limited pulse duration. This ultrashort UV pulse with 19 μJ energy can be utilized in various applications such as high harmonic generation and frustrated tunneling ionization.

Keywords Non-linear optics, Short pulse generation

Ultrashort-pulse lasers have been developed to investigate several light-matter interactions in real time with high temporal resolution[1–4]. In fact, they have been used to capture moments of material changes, such as above-threshold ionization and high-harmonic generation (HHG), where the atomic state is changed within a half-cycle pulse[5–10]. In particular, ultrashort laser pulses in the ultraviolet (UV) region facilitate the study of phonon vibrational modes that require high photon energies. As a useful tool for nonlinear time-resolved spectroscopy in the UV region, they have been utilized to investigate ultrafast electronics and vibrational dynamics in molecules and graphene with high bandgaps[11–13] and to observe fast charge-carrier dynamics in semiconductors on a femtosecond time scale. Furthermore, an ultrashort UV pulse enables high-yield HHG signal generation and frustrated tunneling ionization, which is useful for studying the atomic dynamics of the Rydberg state near the ionization energy of a material[14–17].

One of the most common methods for generating ultrashort UV pulses is spectral broadening through propagation in a gas-filled hollow-core fiber[18–21]. Nibbering et al. obtained a 20 fs, 20 μJ UV pulse by first generating a 50 fs, 400 nm UV pulse with 100 μJ energy through frequency doubling of a 32 fs, 800 nm pulse, and then extending its spectral width to 70 nm with an argon-filled hollow-core fiber[22]. However, the UV pulse duration was limited to 20 fs owing to uncompensated higher-order dispersions. Later, Liu et al. generated a sub 10 fs, 400 nm UV pulse by compensating for higher-order dispersions using chirped mirrors. But the final pulse energy was as low as 4 μJ due to significant energy loss caused by the chirped mirrors with limited spectral bandwidths and several aluminum-coated mirrors[23]. Recently, Travers et al. generated ultrashort UV pulses with high energy of 16 μJ through a soliton self-compression using resonant dispersive-wave emission in a gas-filled hollow-core fiber stage without chirped mirrors[24]. The soliton self-compression fiber stage requires a long space due to a long hollow-core fiber as well as elaborate handling of a beam pointing and a gas pressure for its stable operation. Thus, an efficient method for generating a high-energy ultrashort UV pulse needs to be implemented handily on a small scale for facilitating expansion of its application scope.

A synthesis method was used to generate an ultrashort laser pulse[25]. Krauss et al. obtained a 4.3 fs infrared (IR) pulse by synthesizing two longer IR pulses with different central wavelengths. Here a 7.8 fs IR pulse with a spectral range from 900 to 1400 nm and a 31 fs IR pulse with a spectral range from 1600 to 2000 nm were generated using highly nonlinear fibers, and they were temporally synthesized using a variable delay line. This synthesis method can be applied for the generation of ultrashort UV pulses. First, longer UV pulses can be generated through frequency doubling of an IR pulse in inline multiple nonlinear crystals with different phase-matching conditions, and an ultrashort UV pulse can be obtained by synthesizing longer UV pulses through their temporal matching. In this inline configuration, there is no instability induced by temporal jitters among longer UV pulses during their synthesis. Furthermore, chirped mirrors for dispersion control are not required; thus, the energy loss induced by them can be avoided. But, there will be a limit to energy scalability due to the limit of the size of the nonlinear crystal because the crystal must grow in size to prevent its optical damage as the seed IR pulse energy increases. Consequently, this inline synthesis method is efficient for obtaining high-

[1]Center for Relativistic Laser Science, Institute for Basic Science, Gwangju 61005, Korea. [2]Advanced Photonics Research Institute, Gwangju Institute of Science and Technology, Gwangju 61005, Korea. [3]Department of Physics and Photon Science, Gwangju Institute of Science and Technology, Gwangju 61005, Korea. ✉email: sungjh@gist.ac.kr

energy ultrashort pulses in the UV region, and can be implemented with a compact setup composed of multiple nonlinear crystals.

In this letter, we present an inline synthesizer for generating high-energy sub-5 fs pulses in the UV region. Three nonlinear crystals were serially placed in the propagation path of a broadband IR laser pulse to generate UV pulses with different central wavelengths through second-harmonic (SH) generation. A 4.7 fs UV pulse was obtained by synthesizing three SH signals through the time delay adjustment of each SH signal. Time-delay adjustments were enabled by controlling the relative positions of the nonlinear crystals. Here the temporal waveform of the synthesized UV pulse could be manipulated easily just through the time delay adjustment. This synthesis of SH signals obviates the need for several chirped mirrors for dispersion compensation, resulting in a low energy loss. The waveform of the synthesized UV pulse was measured and its characteristics were investigated by conducting an HHG experiment.

Results

An ultrashort UV pulse can be obtained by generating SH pulses with UV central wavelengths and then synthesizing them in the time domain. SH pulses with different central wavelengths were obtained by adjusting the phase-matching bandwidth of each nonlinear crystal. Temporal coincidence of SH pulses can be achieved by precisely controlling their temporal delays. To achieve efficient temporal coincidence, a close quantitative analysis of the time lags among them should be prioritized.

The time delays of the SH signals from the nonlinear crystals were calculated analytically. Beta-barium borate (BBO) crystals were used as nonlinear crystals to generate SH signals. Three BBO crystals with thicknesses of L_1, L_2 and L_3 were arranged in succession to generate SH signals with central wavelengths of λ_1, λ_2 and λ_3, respectively. The phase delay as well as the group delay of each SH signal has a decisive effect on the temporal waveform of the synthesized pulse. Here the phase delay could be adjusted just through fine tuning of the group delay. The group delay of each SH signal immediately after the third crystal can be expressed as

$$\begin{aligned}
\tau_{\lambda_1} &= \frac{L_1}{v_{BBO_1}(\lambda_1)} + \frac{L_{1,2}}{v_{air}(\lambda_1)} + \frac{L_2}{v_{BBO_2}(\lambda_1)} + \frac{L_{2,3}}{v_{air}(\lambda_1)} + \frac{L_3}{v_{BBO_3}(\lambda_1)}, \\
\tau_{\lambda_2} &= \tau_{2\lambda_2} + \frac{L_2}{v_{BBO_2}(\lambda_2)} + \frac{L_{2,3}}{v_{air}(\lambda_2)} + \frac{L_3}{v_{BBO_3}(\lambda_2)}, \\
\tau_{\lambda_3} &= \tau_{2\lambda_3} + \frac{L_3}{v_{BBO_3}(\lambda_3)}
\end{aligned} \tag{1}$$

Here $\tau_{2\lambda_n}$ is the time delay of the fundamental partial pulse with a central wavelength of $2\lambda_n$ before the nth BBO crystal. $\tau_{2\lambda_1}$ was set to be zero because the origin of the time-frame was the position of the fundamental partial pulse with a central wavelength of $2\lambda_1$ before the first BBO crystal. $v_{BBO_m}(\lambda_n)$ is the group velocity of the SH signal with a central wavelength of λ_n during passage through the mth BBO crystal along the extraordinary axis. $v_{air}(\lambda_n)$ is the group velocity of the SH signal with a central wavelength of λ_n in air. $L_{1,2}(L_{2,3})$ is the separation between the first (second) and second (third) BBO crystal in air. The time delays of the SH signals after the third BBO crystal were predicted using analytical calculations, as shown in Fig. 1. When the fundamental chirp-free pulse passes through the first BBO crystal, an SH signal with a central wavelength of $\lambda_1(\mathrm{UV}_1\ \mathrm{signal})$ is generated. An SH signal with a central wavelength of $\lambda_2(\mathrm{UV}_2\ \mathrm{signal})$ is generated after the second BBO crystal and it will precede or lag behind the UV_1 signal immediately after the second BBO crystal according to the air separation distance of $L_{1,2}$. Similarly, an SH signal with a central wavelength of $\lambda_3(\mathrm{UV}_3\ \mathrm{signal})$ precedes or lags behind the UV_1 signal and the UV_2 signal immediately after the third BBO crystal. As a result, the temporal delays of the three UV signals vary according to the air lengths $L_{1,2}$ and $L_{2,3}$, and the temporal profile of a synthesized UV pulse depends on the air lengths.

A few-cycle IR pulse with a central wavelength of 730 nm was generated using a gas-filled hollow-core fiber. A 25 fs, 1.2 mJ laser pulse from a 1 kHz Ti:sapphire laser was focused at the entrance of the hollow-core fiber with an inner diameter of 500 μm and a length of 2 m, as shown in Fig. 2. Its spectral width was broadened through a self-phase modulation effect in the pressure-gradient neon-filled hollow-core fiber, as shown in Fig. 3a. The broadband laser pulse was collimated after a spherical mirror, and its second-order dispersion was compensated

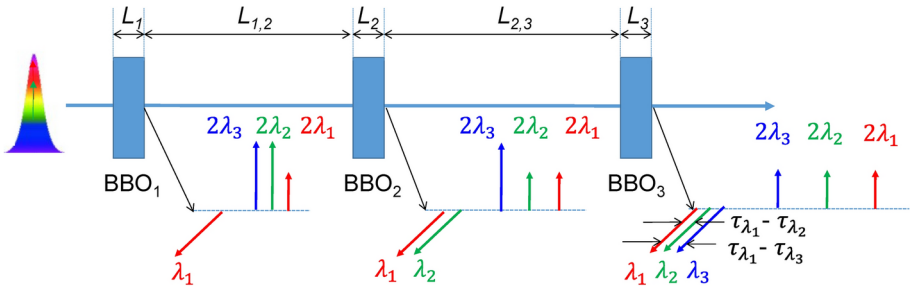

Fig. 1. Time delays of spectral components of the fundamental signal and the second-harmonic signals in inline UV pulse synthesizer.

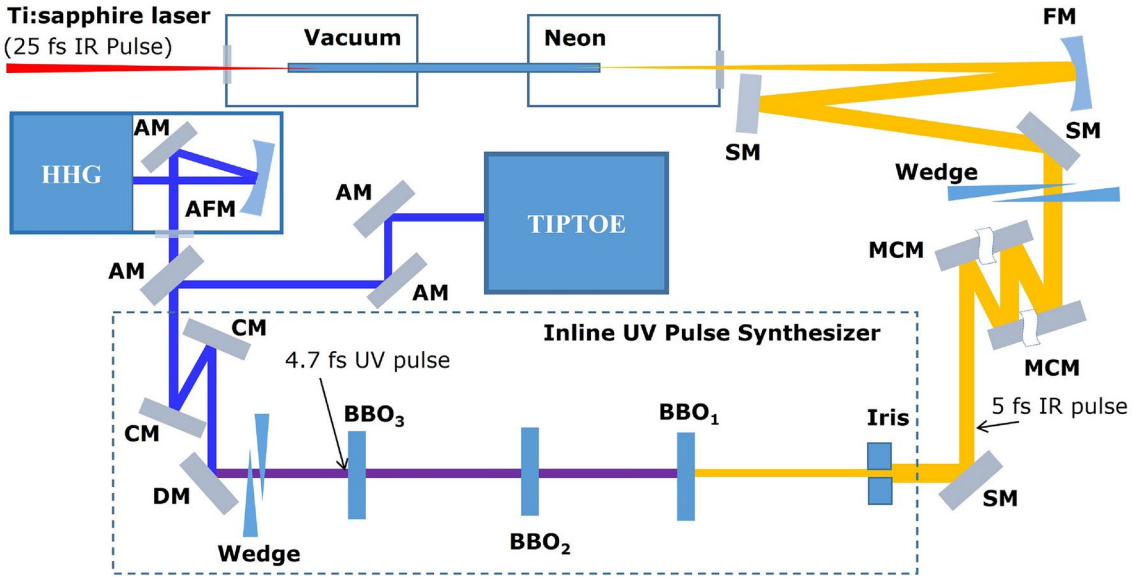

Fig. 2. Experimental setup for synthesized UV pulse generation. *SM* silver mirror, *MCM* multiple chirped mirror, *CM* chirped mirror, *DM* dichroic mirror, *FM* focus mirror, *AM* aluminum mirror, *AFM* aluminum focus mirror.

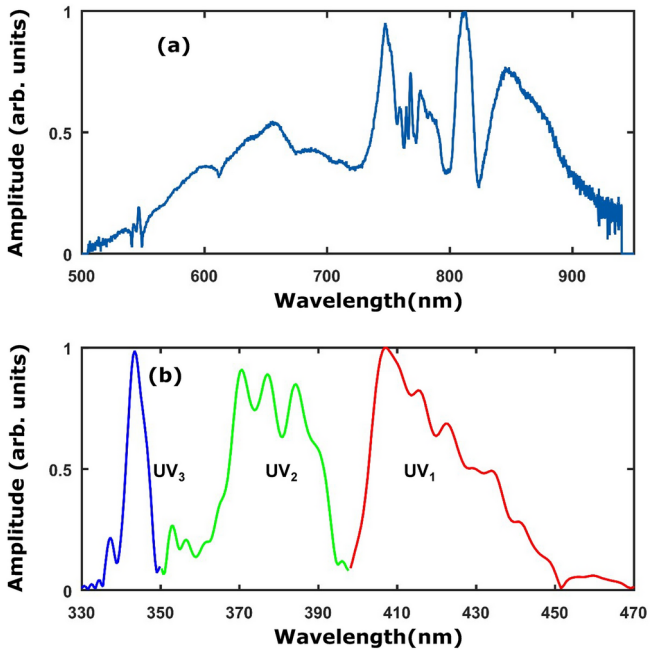

Fig. 3. Measured spectra of (**a**) fundamental input signal and (**b**) second harmonic signal.

using an array of chirp mirrors and one pair of fused silica wedges[26]. Finally, the compressed laser pulse with a 320 μJ energy and a 5 fs duration was used as a broadband seed pulse of an inline UV pulse synthesizer.

The UV pulse synthesizer consists of a single iris, three BBO crystals, a thin wedge pair, a dichroic mirror, and two UV chirp mirrors, as shown in Fig. 2. The iris was used to reduce the beam diameter from 15 mm to 8 mm, considering the 10 mm diameter BBO crystals. After the iris, the laser pulse with 120 μJ energy was made incident to three BBO crystals. The first, second, and third BBO crystals had thicknesses of 100, 100, and 200 μm , respectively. Here the third BBO crystal was thicker than other crystals to increase the conversion efficiency of the UV_3 signal for a low intensity of the fundamental partial pulse with a central wavelength of $2\lambda_3$. UV pulses with central wavelengths of 420, 375, and 345 nm were produced by the SH generation in the first, second, and third BBO crystals, respectively, as shown in Fig. 3b. A thin-wedge pair was used to control the dispersion of the synthesized UV pulse minutely. The synthesized UV pulse, which was separated from the fundamental IR pulse

using a dichroic mirror, was introduced into the target chamber for the HHG experiment or into a temporal characterization device. Two UV chirp mirrors were installed after the dichroic mirror to compensate for the total group delay dispersion originating from the materials, including the thin wedge, window of the target chamber, and air after the third BBO crystal.

The waveform of the synthesized UV pulse immediately after the third BBO crystal is theoretically calculated to estimate the temporal profile. The optical waveform can be described as follows:

$$f(t,t_1,t_2)=\frac{1}{3}\left\{\exp\left(-\frac{2\log(2)t^2}{\tau_1^2}\right)\exp\left(\frac{i2\pi c}{\lambda_1}t\right)+\exp\left(-\frac{2\log(2)(t-t_1)^2}{\tau_2^2}\right)\exp\left(\frac{i2\pi c}{\lambda_2}(t-t_1)\right)\right.$$
$$\left.+\exp\left(-\frac{2\log(2)(t-t_2)^2}{\tau_3^2}\right)\exp\left(\frac{i2\pi c}{\lambda_3}(t-t_2)\right)\right\} \quad (2)$$

where $t_1(t_2)$ represents the time delay of the UV_2 signal (UV_3 signal) with respect to the UV_1 signal. τ_1, τ_2 and τ_3 represent the temporal durations of UV_1 signal, UV_2 signal and UV_3 signal, respectively. To prioritize the temporal coincidence between the UV_1 signal and UV_3 signal, the separation distance between the first and third BBO crystals was calculated to be approximately 210 mm. Under the condition of temporal coincidence between the UV_1 signal and UV_3 signal, the temporal profile of the synthesized pulse was sensitive to the relative position of the second BBO crystal, which determined the temporal lag between the UV_1 signal and UV_2 signal, as shown in Fig. 4. Consequently, the separation distance between the three BBO crystals had a decisive effect on the temporal profile of the synthesized pulse.

The temporal profile of the synthesized UV pulse was measured using tunneling ionization with perturbation for the time-domain observation of an electric field (TIPTOE) device[27]. First, the temporal durations of UV_1 signal, UV_2, and UV_3 signals were 12, 20, and 30 fs, respectively. Figure 4 shows the temporal profiles measured according to the time delay between the UV_1 signal and UV_2 signal when the UV_1 signal and UV_3 signal were synthesized. When the time delay between the UV_1 signal and the UV_2 signal was set to zero and the separation distance between the first and second BBO crystals was approximately 100 mm, the temporal profile of the synthesized UV pulse was optimized, as shown in Fig. 4a. Here the pulse duration was measured to be 4.7 fs (FWHM). At a small time delay (0.65 fs corresponding to a separation distance of 124 mm), the temporal profile deviated significantly from the optimized one, resulting in double peaks, as shown in Fig. 4b. At a time delay of 1.3 fs corresponding to a separation distance of 148 mm, the temporal profile approached the optimized profile,

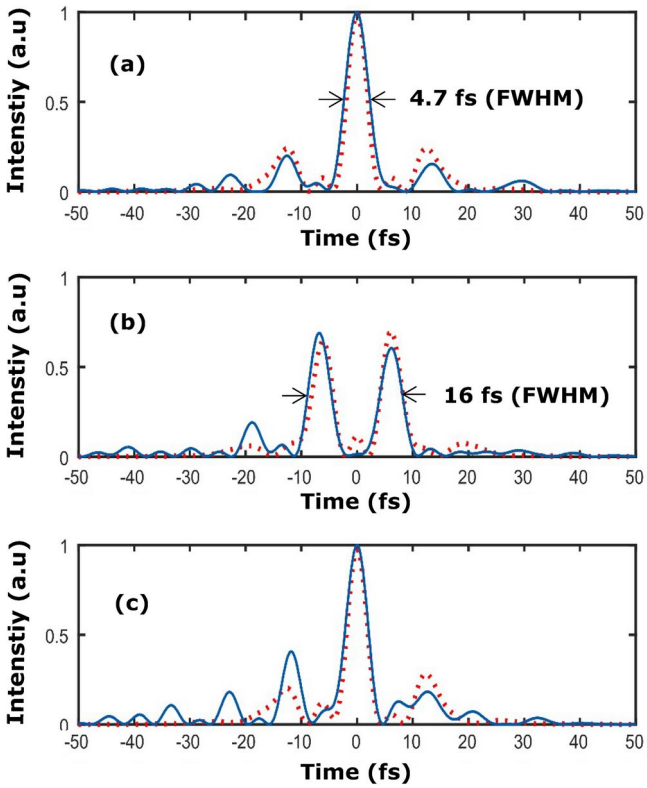

Fig. 4. Measured temporal intensity profiles (solid blue line) and calculated profiles (dotted red line) of the synthesized pulse when time delays between the first and second UV pulse were (**a**) zero, (**b**) 0.65 fs and (**c**) 1.3 fs under temporal coincidence between the first and the third UV pulse.

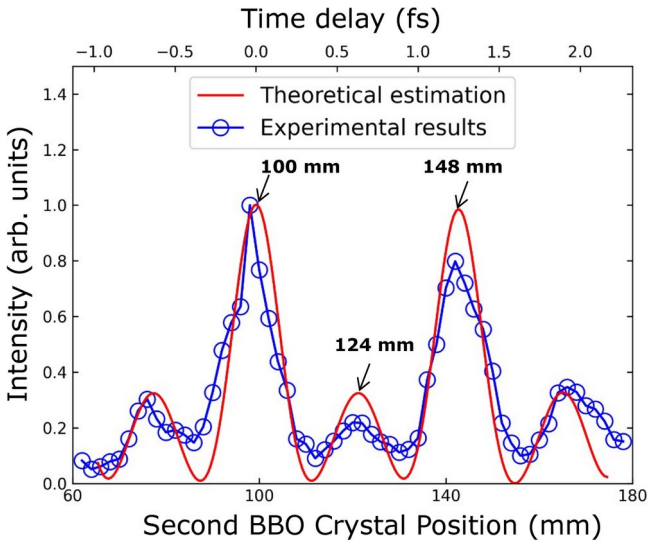

Fig. 5. Air ionization rate depending on time delay between the first UV signal and the second UV signal under temporal coincidence between the first and the third UV pulse.

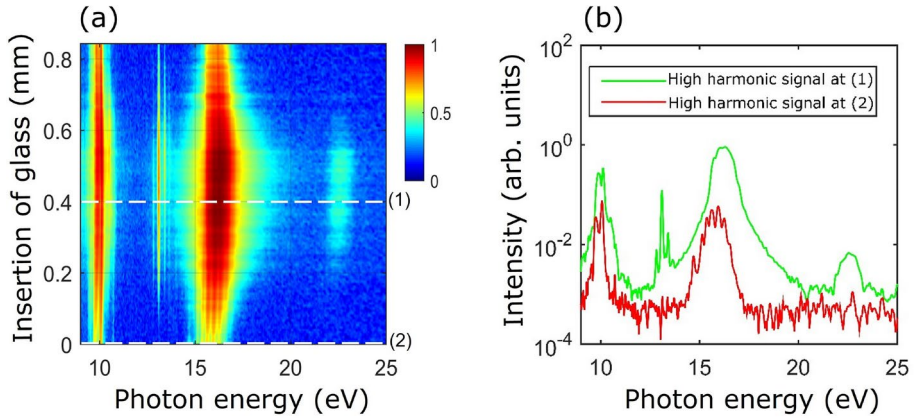

Fig. 6. Measured spectra of high harmonic signals as a function of insertion length of glass wedge when synthesized UV pulses were focused into a krypton gas target.

as shown in Fig. 4c. The adjustment range of the time delay between the UV_1 signal and the UV_2 signal for temporal optimization of the synthesized UV pulse was of the order of an optical cycle at the central wavelength of the fundamental IR pulse. These measured profiles, which agree well with the calculated profiles, show that the temporal profile of the synthesized UV pulse can be controlled by adjusting the relative positions of the BBO crystals.

The rate of air ionization induced by the synthesized UV pulses was measured using a TIPTOE device with no perturbation signal channel[27]. The synthesized UV pulse was focused on the air gap between the copper plates of the TIPTOE device and the air ionization rate was measured. The air ionization rate, which is proportional to the integral value of the 8th power of the incident optical waveform, can be calculated by using the Equation (2)[28]. Figure 5 shows the air ionization rate as a function of the position of the second BBO crystal relative to that of the first BBO crystal under temporal coincidence between the UV_1 signal and UV_3 signal. The measured air ionization rate agreed well with the calculated rate. Consequently, inline UV pulse synthesis is demonstrated to be a reliable method for generating ultrashort UV pulses.

An HHG experiment was conducted to prove the utility of the synthesized sub-5 fs UV pulses. At first, the synthesized UV pulse with a 19 μJ energy was directed at a vacuum chamber for the HHG experiment. The temporal profile was controlled by varying the insertion length of the glass wedge. Figure 6a shows the spectra of the HHG signals measured as a function of the insertion length of the glass wedge when the synthesized UV pulses were focused onto a krypton gas target in the vacuum chamber. When the insertion length was 0.4 mm, the temporal profile of the synthesized UV pulse was optimized and its HHG signal was observed up to 23 eV, as shown by the green line of Fig. 6b. In contrast, when the insertion length was approximately 0 mm, the synthesized UV pulse with a negative chirp had few peaks, and its HHG signal was observed up to 17 eV

owing to its lower peak intensity, as shown by the red line in Fig. 6b. This experimental result shows that the synthesized UV pulse can be efficiently utilized to generate HHG signals, the characteristics of which depend on the temporal profile of the synthesized UV pulse.

Conclusion

In conclusion, we demonstrated the inline synthesis of three UV pulses with central wavelengths of 420, 375, and 345 nm to generate a high-energy sub-5 fs UV pulse. The synthesized UV pulse was generated through three BBO crystals with different phase-matching conditions, and the waveform was controlled by adjusting the relative positions of the three crystals. The temporal waveform of the synthesized UV pulse was measured using a TIPTOE device, with a minimum duration of 4.7 fs. This 4.7 fs UV pulse with a 19 μJ energy was efficiently utilized in the HHG experiment. To the best of our knowledge, this inline UV pulse synthesis is the first synthesis technique applied to the UV region. We anticipate that this inline synthesis method will be highly effective for generating high-energy ultrashort UV pulses and useful for studying atomic dynamics in the UV region.

Data availability

All data generated or analyzed during this study are included in this published article.

Received: 22 July 2024; Accepted: 4 October 2024
Published online: 18 October 2024

References

1. Brabec, T. & Krausz, F. Intense few-cycle laser fields: Frontiers of nonlinear optics. *Rev. Mod. Phys.* **72**, 545–591 (2000).
2. Dudovich, N. et al. Measuring and controlling the birth of attosecond XUV pulses. *Nat. Phys.* **2**, 781–786 (2006).
3. Corkum, P. B. & Krausz, F. Attosecond science. *Nat. Phys.* **3**, 381–387 (2007).
4. Goulielmakis, E. et al. Single-cycle nonlinear optics. *Science* **320**, 1614–1617 (2008).
5. Corkum, P. B. Plasma perspective on strong field multiphoton ionization. *Phys. Rev. Lett.* **71**, 1994–1997 (1993).
6. McPherson, A. et al. Studies of multiphoton production of vacuum-ultraviolet radiation in the rare gases. *J. Opt. Soc. Am. B* **4**, 595–601 (1987).
7. Macklin, J. J., Kmetec, J. D. & Gordon, C. L. High-order harmonic generation using intense femtosecond pulses. *Phys. Rev. Lett.* **70**, 766–769 (1993).
8. Chang, Z., Rundquist, A., Wang, H., Murnane, M. M. & Kapteyn, H. C. Generation of coherent soft x rays at 2.7 nm using high harmonics. *Phys. Rev. Lett.* **79**, 2967–2970 (1997).
9. Spielmann, C. et al. Generation of coherent x-rays in the water window using 5-femtosecond laser pulses. *Science* **278**, 661–664 (1999).
10. Agostini, P., Fabre, F., Mainfray, G., Petite, G. & Rahman, N. K. Free-free transitions following six-photon ionization of xenon atoms. *Phys. Rev. Lett.* **42**, 1127–1130 (1979).
11. Liu, J., Okamura, K., Kida, Y., Teramoto, T. & Kobayashi, T. Clean sub-8-fs pulses at 400 nm generated by a hollow fiber compressor for ultraviolet ultrafast pump-probe spectroscopy. *Opt. Express* **18**, 20645–20650 (2010).
12. Oum, K. et al. Observation of ultrafast carrier dynamics and phonon relaxation of graphene from the deep-ultraviolet to the visible region. *J. Phys. Chem. C* **118**, 6454–6461 (2014).
13. Hertel, I. V. & Radloff, W. Ultrafast dynamics in isolated molecules and molecular clusters. *Rep. Prog. Phys.* **69**, 1897 (2006).
14. Nubbemeyer, T., Gorling, K., Saenz, A., Eichmann, U. & Sandner, W. Strong-field tunneling without ionization. *Phys. Rev. Lett.* **101**, 233001 (2008).
15. Eichmann, U., Saenz, A., Eilzer, S., Nubbemeyer, T. & Sandner, W. Observing rydberg atoms to survive intense laser fields. *Phys. Rev. Lett.* **110**, 203002 (2013).
16. Yun, H. et al. Coherent extreme-ultraviolet emission generated through frustrated tunnelling ionization. *Nat. Photonics* **12**, 620–624 (2018).
17. Li, Y., Xu, J., Yu, B. & Wang, X. Frustrated double ionization of atoms in strong laser fields. *Opt. Express* **28**, 7341–7349 (2020).
18. Backus, S., Asaki, M. T., Shi, C., Kapteyn, H. C. & Murnane, M. M. Intracavity frequency doubling in a ti:sapphire laser: generation of 14-fs pulses at 416 nm. *Opt. Lett.* **19**, 399–401 (1994).
19. Ashworth, S. H., Joschko, M., Woerner, M., Riedle, E. & Elsaesser, T. Generation of 16-fs pulses at 425 nm by extracavity frequency doubling of a mode-locked ti:sapphire laser. *Opt. Lett.* **20**, 2120–2122 (1995).
20. Zhavoronkov, N. & Korn, G. Generation of single intense short optical pulses by ultrafast molecular phase modulation. *Phys. Rev. Lett.* **88**, 203901 (2002).
21. Zhou, X., Kanai, T., Yoshitomi, D., Sekikawa, T. & Watanabe, S. Generation of high average power, 7.5-fs blue pulses at 5 kHz by adaptive phase control. *Appl. Phys. B* **81**, 13–17 (2005).
22. Nibbering, E. T. J., Dühr, O. & Korn, G. Generation of intense tunable 20-fs pulses near 400 nm by use of a gas-filled hollow waveguide. *Opt. Lett.* **22**, 1335–1337 (1997).
23. Liu, J., Kida, Y., Teramoto, T. & Kobayashi, T. Generation of stable sub-10 fs pulses at 400 nm in a hollow fiber for UV pump-probe experiment. *Opt. Express* **18**, 4664–4672 (2010).
24. Travers, J. C., Grigorova, T. F., Brahms, C. & Belli, F. High-energy pulse self-compression and ultraviolet generation through soliton dynamics in hollow capillary fibres. *Nat. Photonics* **13**, 547–554 (2019).
25. Krauss, G. et al. Synthesis of a single cycle of light with compact erbium-doped fibre technology. *Nat. Photonics* **4**, 33–36 (2010).
26. Hwang, S. I. et al. Generation of a single-cycle pulse using a two-stage compressor and its temporal characterization using a tunnelling ionization method. *Sci. Rep.* **9**, 1613 (2019).
27. Park, S. B. et al. Direct sampling of a light wave in air. *Optica* **5**, 402–408 (2018).
28. Cho, W., Shin, J.-U. & Kim, K. T. Reconstruction algorithm for tunneling ionization with a perturbation for the time-domain observation of an electric-field. *Sci. Rep.* **11**, 13014 (2021).

Acknowledgements

This work was supported by the Institute for Basic Science (IBS-R012-D1) and the Ultrashort Quantum Beam Facility operation program (No. 140011) through Advanced Photonics Research Institute, Gwangju Institute of Science and Technology.

Author contributions

Wosik Cho provided assistance of optical waveform measurement based on the TIPTOE , while Hyeok Yun provided helps for the high harmonic generation experiements. Kyung Taec Kim, Jin Woo Yun and Seong Ku Lee gave valuable advice for the manuscript. Sung In Hwang and Jae Hee Sung performed data analysis and wrote the manuscript.

Declarations

Competing interests

The authors declare no competing interests.

Additional information

Correspondence and requests for materials should be addressed to J.H.S.

Reprints and permissions information is available at www.nature.com/reprints.

Publisher's note Springer Nature remains neutral with regard to jurisdictional claims in published maps and institutional affiliations.